Geometric Vacuum Selection from Constrained Spacetime Foliations

Michael Spina
michael.spina@mail.com

February 18, 2026

Abstract

We investigate a scalar-field framework for vacuum structure in General Relativity, in which the foliation defined by the gradient of a time-ordering field Θ is subject to a non-local geometric constraint. The level sets $\Theta = \text{const}$ define spacelike hypersurfaces interpreted as physical "present" leaves. The constraint fixes the asymptotic normalized average of the squared extrinsic curvature to a constant scale K_0^2, enforced by a leafwise Lagrange multiplier.

We show that this condition acts as a vacuum-selection principle: in the infrared limit it generically excludes Minkowski and selects de Sitter, with expansion rate fixed by $H^2 = K_0^2/3$. The same infrared mechanism guarantees recovery of local GR (Schwarzschild and post-Newtonian regimes), since non-local corrections are volume-suppressed.

We then complete the covariant variational and perturbative analysis. At the variational level, we derive explicit bulk+boundary contributions for the leafwise functionals and for $\delta^2(I_1/I_0)$, including boundary shape-derivative terms. At the perturbative level, we construct the full tensor/vector/scalar quadratic operator, its 4D spin-projector inversion, dispersion relations, and residues, with explicit IR scaling checks. Finally, we provide an operational EFT validity analysis: nonlocal corrections remain small in the tested domain, no strong-coupling signal appears in the adopted proxies, and positive dispersion is verified up to the tested scale $q^2 \leq 4$ (operational cutoff, not fundamental UV cutoff).

Conventions

We work in natural units $c = \hbar = 1$ adopting metric signature $(+,-,-,-)$. Our curvature conventions follow

$$R^{\rho}{}_{\sigma\mu\nu} = \partial_\mu \Gamma^{\rho}_{\nu\sigma} - \partial_\nu \Gamma^{\rho}_{\mu\sigma} + \Gamma^{\rho}_{\mu\lambda}\Gamma^{\lambda}_{\nu\sigma} - \Gamma^{\rho}_{\nu\lambda}\Gamma^{\lambda}_{\mu\sigma}, \qquad R_{\mu\nu} = R^{\rho}{}_{\mu\rho\nu}. \tag{1}$$

For the nonlocal functional we set the smoothing/window parameter to its default value $W = 1$ throughout (no variation with respect to W is performed).

1 Motivation and scope

General Relativity provides an accurate local description of gravitational phenomena, yet it leaves the global structure of time and the selection of the vacuum largely unconstrained. In particular, both Minkowski and de Sitter spacetimes are admissible vacuum solutions, despite their radically different global properties. The observed accelerated expansion is therefore introduced phenomenologically through a cosmological constant, rather than emerging from a geometric principle.

In this work we explore a minimal geometric extension of General Relativity based on a scalar field Θ whose timelike gradient defines a preferred foliation of spacetime. Preferred-foliation frameworks closely related in spirit include Einstein–Æther and khronometric theories, where a timelike vector (or scalar-defined) structure selects a preferred slicing while remaining compatible with standard local tests in appropriate limits [1, 2, 3, 4]. The level sets $\Theta = \text{const}$ are interpreted as physical "present" hypersurfaces, providing a global time-ordering structure without affecting local causal relations or observer-dependent simultaneity.

The central ingredient is a non-local geometric constraint acting on the foliation itself: the normalized average of the squared extrinsic curvature K^2 over a causally defined domain on each hypersurface is fixed to a constant value. This leafwise constraint selects the global vacuum geometry without introducing unsuppressed local modifications of the gravitational dynamics.

We show that asymptotically flat Minkowski spacetime is not generically selected as an infrared vacuum, while de Sitter spacetime is admitted as a consistent asymptotic solution, with its expansion rate fixed by the constraint. Local Schwarzschild and post-Newtonian physics are recovered, as the constraint is dominated by infrared scales.

The purpose of this work is to present a complete internal consistency chain for the proposed mechanism: (i) covariant variational control of the non-local leafwise action, (ii) perturbative spectral stability of tensor/vector/scalar sectors, and (iii) an operational EFT validity window. This establishes the framework as a quantitatively testable vacuum-selection model, not only a qualitative sketch. The remaining open front is not internal consistency but phenomenology: observational inference, UV completion, and gauge-independent BRST/Faddeev–Popov closure of the perturbative gauge-fixing sector.

2 Geometric setup

We consider a four-dimensional spacetime $(\mathcal{M}, g_{\mu\nu})$ endowed with a scalar field Θ. When the gradient $\nabla_\mu\Theta$ is timelike, the level sets $\Theta = \text{const}$ define a foliation of spacetime by spacelike hypersurfaces Σ_Θ. Scalar fields used to

define preferred time functions and associated foliations in GR have been considered in earlier contexts; see e.g. [5]. Throughout this work, we restrict attention to configurations satisfying this condition.

The scalar invariant

$$X \equiv g^{\mu\nu}\partial_\mu\Theta\,\partial_\nu\Theta \tag{2}$$

is assumed to be positive, ensuring that $\nabla_\mu\Theta$ is timelike. We then define the unit normal vector field to the foliation as

$$u_\mu \equiv \frac{\partial_\mu\Theta}{\sqrt{X}}\,. \tag{3}$$

The induced metric on each hypersurface Σ_Θ is given by

$$h_{\mu\nu} \equiv g_{\mu\nu} - u_\mu u_\nu, \tag{4}$$

which projects tensors onto directions tangent to the foliation. We denote by γ_{ij} the (positive-definite) induced three-metric on each leaf Σ_Θ. Its determinant is $\gamma \equiv \det(\gamma_{ij})$, and the intrinsic volume element is $\sqrt{\gamma}\,d^3x$. The extrinsic curvature of the hypersurfaces is defined in the standard way as

$$K_{\mu\nu} \equiv h^\alpha{}_\mu h^\beta{}_\nu \nabla_\alpha u_\beta. \tag{5}$$

A key scalar quantity in what follows is the squared extrinsic curvature,

$$K^2 \equiv K_{\mu\nu}K^{\mu\nu}, \tag{6}$$

which measures the curvature of the $\Theta = \text{const}$ hypersurfaces within spacetime. Together with the Ricci scalar R of the spacetime metric, these invariants will enter the action and the geometric constraint introduced in later sections.

3 Spherically symmetric sector

In order to analyze the geometric properties of the Θ-foliation and to construct explicit examples, we consider a static, spherically symmetric spacetime. The metric is written in the form

$$ds^2 = A(r)\,dt^2 - B(r)\,dr^2 - r^2\left(d\vartheta^2 + \sin^2\vartheta\,d\varphi^2\right), \tag{7}$$

where $A(r)$ and $B(r)$ are positive functions of the radial coordinate.

For the scalar field we adopt the ansatz

$$\Theta(t, r) = t + \psi(r), \tag{8}$$

which preserves spherical symmetry while allowing for nontrivial foliations tilted with respect to the static time coordinate. This form captures the most general Θ compatible with the symmetries of the metric.

3.1 Kinematic invariant

For the above ansatz, the kinetic scalar X takes the form

$$X = \frac{1}{A(r)} - \frac{\psi'(r)^2}{B(r)}. \tag{9}$$

The requirement that the foliation be spacelike implies $X > 0$, which constrains the admissible profiles $\psi(r)$.

3.2 Curvature invariants

The Ricci scalar associated with the metric is given by

$$R = R[A(r), B(r)], \tag{10}$$

where the explicit expression, though lengthy, depends only on the radial functions and their derivatives.

The squared extrinsic curvature of the $\Theta = \text{const}$ hypersurfaces can be written as

$$K^2 = K_{\mu\nu}K^{\mu\nu} = K^2\big(A(r), B(r), \psi(r), \psi'(r), \psi''(r)\big). \tag{11}$$

The explicit form is algebraically involved and will not be reproduced in full here. What is important for our purposes is its dependence on the radial coordinate through the functions $A(r)$, $B(r)$ and the foliation profile $\psi(r)$.

These local expressions will enter the construction of the action and the leafwise geometric constraint discussed in the following sections.

4 Constrained action

4.1 Local gravitational dynamics

We start from a local action consisting of the Einstein–Hilbert term and a minimal kinetic term for the scalar field Θ,

$$S_{\text{loc}} = \int d^4x\sqrt{-g}\left[\frac{1}{2\kappa}(R - 2\Lambda) - \frac{\alpha}{2}X\right], \tag{12}$$

where $\kappa = 8\pi G$, Λ is a cosmological constant and $X = g^{\mu\nu}\partial_\mu\Theta\,\partial_\nu\Theta$. We take the scalar field Θ to have dimensions of length (time in units $c = 1$), so that $\partial_\mu\Theta$ is dimensionless and the kinetic scalar X is dimensionless. Accordingly, the coupling constant α has dimensions $[L^{-4}]$. Although the local action includes a standard kinetic term for the scalar field Θ, this term is not introduced to model an additional physical scalar degree of freedom. Rather, Θ plays the role of a geometric time-ordering field whose gradient defines the spacetime foliation on which the non-local constraint acts.

The kinetic term should therefore be understood as a regulator enforcing the timelike character of $\nabla_\mu\Theta$ and the regularity of the foliation. In the infrared regime of interest, the dynamics of Θ is dominated by the leafwise constraint, and the theory approaches a non-propagating, cuscuton-like limit. The perturbative scalar/vector/tensor mode content is now explicitly analyzed in the repository pipeline `Paper/Perturbative_Spectrum_Study/scripts/00_tensor_channel_ir_stability.wl`– `Paper/Perturbative_Spectrum_Study/scripts/15_eft_validity_scales_proxy.wl`, including kinetic/gradient conditions, full dispersion relations, and residue checks. This local action is fully diffeomorphism invariant and does not introduce any preferred frame by itself.

On the bare cosmological constant. We keep Λ explicit for generality. In the vacuum-selection discussion below we set the bare value to $\Lambda = 0$, so that the de Sitter curvature scale arises from the leafwise constraint as a selection rule rather than being put in by hand.

4.2 Leafwise geometric constraint

The defining ingredient of the theory is a non-local geometric constraint acting on the foliation defined by Θ. For each hypersurface Σ_Θ we consider a causally defined domain $D_\Theta \subset \Sigma_\Theta$, determined by the spacetime geometry and the foliation itself.

Throughout this work, the causal domain D_Θ is defined as the maximal causally accessible region of the hypersurface Σ_Θ, i.e. the largest connected subset of Σ_Θ whose points are mutually related by causal curves in the ambient spacetime geometry. This definition is intrinsic to the foliation and does not depend on the choice of any fiducial observer. In asymptotically flat spacetimes, D_Θ extends to spatial infinity, while in spacetimes with a cosmological horizon the causal domain is bounded by the horizon scale, providing a finite and geometrically natural infrared cutoff.

On each leaf we define the functionals

$$I_0[\Theta] \equiv \int_{D_\Theta} W\,\sqrt{\gamma}\,d^3x, \qquad I_1[\Theta] \equiv \int_{D_\Theta} W\,K^2\sqrt{\gamma}\,d^3x, \tag{13}$$

where γ is the determinant of the induced three-metric γ_{ij} on Σ_Θ, and $W \geq 0$ is an optional smoothing/window weight (set to $W = 1$ in this work). Then

$$\langle K^2\rangle_{D_\Theta} \equiv \frac{I_1[\Theta]}{I_0[\Theta]}. \tag{14}$$

The geometric constraint is imposed by requiring

$$\lim_{R\to\infty} \frac{\int_{D_\Theta(R)} K^2\sqrt{\gamma}\,d^3x}{\int_{D_\Theta(R)} \sqrt{\gamma}\,d^3x} = K_0^2, \tag{15}$$

where K_0 is a fixed parameter setting the curvature scale of the foliation. Here, $D_\Theta(R)$ denotes a family of nested subdomains monotonically exhausting D_Θ as $R \to \infty$. In spacetimes where D_Θ is itself bounded (e.g. by a cosmological horizon), the limit is saturated at finite R and the constraint is automatically well-defined without external regulators. Conceptually, the use of global (or nonlocal) constraints to control vacuum properties has precedents in unimodular formulations and vacuum-energy sequestering mechanisms[1]. The present constraint, however, acts on a foliation-dependent extrinsic-curvature functional rather than on the metric determinant or on matter-sector vacuum contributions.s.

4.3 Full action

The constraint is enforced through a Lagrange multiplier $\lambda(\Theta)$ that depends only on the value of the scalar field and is therefore constant on each hypersurface Σ_Θ. The full action reads

$$S = S_{\rm loc} + \int d\Theta\, \lambda(\Theta) \left[I_1[\Theta] - K_0^2 I_0[\Theta] \right]. \tag{16}$$

With $[\Theta] = L$, the leafwise Lagrange multiplier $\lambda(\Theta)$ has dimensions $[L^{-2}]$, ensuring that the non-local contribution to the action is dimensionless. Because λ is not a local field but a function of Θ only, the constraint does not generate a pointwise equation $K^2(x) = K_0^2$. Instead, it acts globally on the geometry of each leaf, selecting admissible foliations without introducing unsuppressed local modifications of the gravitational dynamics. Boundary terms required for a well-defined variational principle are assumed implicitly.

4.4 Variational structure and infrared dominance

The variational structure of the non-local action (16) is now implemented explicitly in covariant 4D form in the `Paper/Variational_Derivation/` pipeline. At first order one obtains the bulk+boundary split

$$\delta I_0 = \int d^4x\, \chi\, \delta\mu + \int d^4x\, \mu\, \delta\chi, \tag{17}$$

$$\delta I_1 = \int d^4x\, \chi K^2\, \delta\mu + \int d^4x\, \chi\mu\, \delta K^2 + \int d^4x\, \mu K^2\, \delta\chi, \tag{18}$$

which yields

$$\delta\left(\frac{I_1}{I_0}\right) = \frac{I_0\, \delta I_1 - I_1\, \delta I_0}{I_0^2}. \tag{19}$$

At second order, the ratio expansion is validated in the perturbative pipeline:

$$\delta^2 Q = \frac{\delta^2 I_1 - q\, \delta^2 I_0}{I_0} - 2\, \frac{\delta I_0 \left(\delta I_1 - q\, \delta I_0\right)}{I_0^2}, \qquad q \equiv \frac{I_1}{I_0}. \tag{20}$$

[1] ...

Projected on mode vectors this gives the quadratic kernel used in the full perturbative sector,

$$q_{\text{kernel}} = \frac{B - qA}{I_0} - \frac{a\,(b - qa)^T + (b - qa)\,a^T}{I_0^2}, \tag{21}$$

derived first-principles in the same computational chain.

Boundary-shape terms are explicitly controlled. For moving finite domains $R \to R + \epsilon\rho + \epsilon^2\sigma/2$ one gets $\delta\chi = \rho\,\delta(r - R)$ and the expected second-order distributional term, verified against Leibniz differentiation in dedicated boundary-shape tests. Finite-domain ratio and constraint checks show machine-precision agreement between analytic formulas and independent finite-difference estimates.

Quantitatively, the non-local response scales as $\sim 1/I_0$ (in tests $I_0 \sim L^3$, hence $\sim L^{-3}$), as documented by the variational and perturbative IR-scaling checks. This provides an explicit variational basis for local GR recovery and for the infrared dominance mechanism used throughout the manuscript.

5 Sanity checks and local GR recovery

5.1 Schwarzschild test

As a first consistency check, we evaluate the curvature invariants for the Schwarzschild solution,

$$A(r) = 1 - \frac{2M}{r}, \qquad B(r) = \left(1 - \frac{2M}{r}\right)^{-1}. \tag{22}$$

The Ricci scalar vanishes identically,

$$R\big|_{\text{Schw}} = 0, \tag{23}$$

as expected for a vacuum solution of General Relativity. Crucially, the existence of this solution is not obstructed by the leafwise constraint. Since the geometric condition (15) is defined as an asymptotic limit $R \to \infty$, the contributions from local matter distributions or compact objects like black holes are suppressed by the infinite volume of the integration domain. Consequently, the theory does not introduce unsuppressed local modifications of the gravitational dynamics. The recovery of standard weak-field and post-Newtonian behavior in the presence of preferred-structure fields follows from this infrared dominance, analogous to established results in Einstein–Æther theory; see e.g. [2] for explicit equivalence proofs

5.2 Static foliation limit

When the foliation coincides with constant-t hypersurfaces ($\psi = \text{const}$), the scalar invariants reduce to

$$X\big|_{\psi'=0} = \frac{1}{A(r)}, \tag{24}$$

$$K^2\big|_{\psi'=0} = 0. \tag{25}$$

In this static limit, the extrinsic curvature of the Θ-hypersurfaces vanishes identically. However, compatibility with General Relativity holds more generally. For generic asymptotically flat foliations where K^2 may be non-vanishing near the source, the contribution to the global average scales as the ratio of a finite strong-field volume to the infinite integration volume. In the limit $R \to \infty$, local sources effectively represent measure-zero corrections to the vacuum selection rule. This confirms that the global constraint acts purely as an infrared boundary condition, leaving local astrophysical tests of gravity unaffected. The static identities above are also certified in the Lean artifact by the static-limit lemmas in `StaticSanityCheck/StaticLimit.lean`.

6 Vacuum selection from the leafwise constraint

6.1 Minkowski spacetime

We now evaluate the leafwise geometric functional for Minkowski spacetime, written in static spherical coordinates,

$$A(r) = 1, \qquad B(r) = 1. \tag{26}$$

For foliations of the form $\Theta = t + \psi(r)$ the kinetic invariant becomes

$$X = 1 - \psi'(r)^2, \tag{27}$$

so that the timelike condition requires $|\psi'(r)| < 1$.

For a linear tilt $\psi(r) = vr$, one finds

$$K^2(r) = \frac{2v^2}{r^2(1-v^2)}, \tag{28}$$

which is strictly positive but decays as r^{-2} at large radius.

6.2 Infrared behaviour of the leafwise average

The leafwise constraint does not involve the pointwise value of $K^2(r)$, but its normalized average over a causally defined domain D_Θ,

$$\langle K^2 \rangle_{D_\Theta} = \frac{\int_{D_\Theta} W\, K^2 \sqrt{\gamma}\, d^3x}{\int_{D_\Theta} W\, \sqrt{\gamma}\, d^3x}. \tag{29}$$

In Minkowski spacetime, the induced volume element grows as $\sqrt{\gamma} \sim r^2$, while $K^2 \sim r^{-2}$. As a consequence, the numerator scales linearly with the infrared cutoff, whereas the denominator grows cubically. In the infrared limit one therefore finds

$$\langle K^2 \rangle_{D_\Theta} \xrightarrow{\text{IR}} 0. \tag{30}$$

In Lean, this infrared statement is certified by the Minkowski IR-limit theorem in `StaticSanityCheck/MinkowskiLinearTilt.lean`.

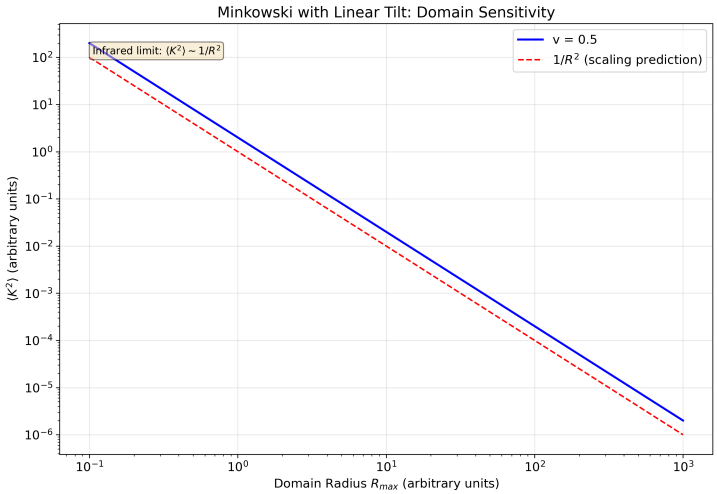

Figure 1: Infrared behaviour of the leafwise average $\langle K^2 \rangle$ in Minkowski spacetime with linear tilt. The numerical scaling confirms $\langle K^2 \rangle \propto R_{\max}^{-2}$, implying a vanishing average extrinsic-curvature invariant in the infrared limit $R_{\max} \to \infty$.

This result holds independently of the tilt parameter v and reflects a purely geometric scaling property of asymptotically flat spacetime.

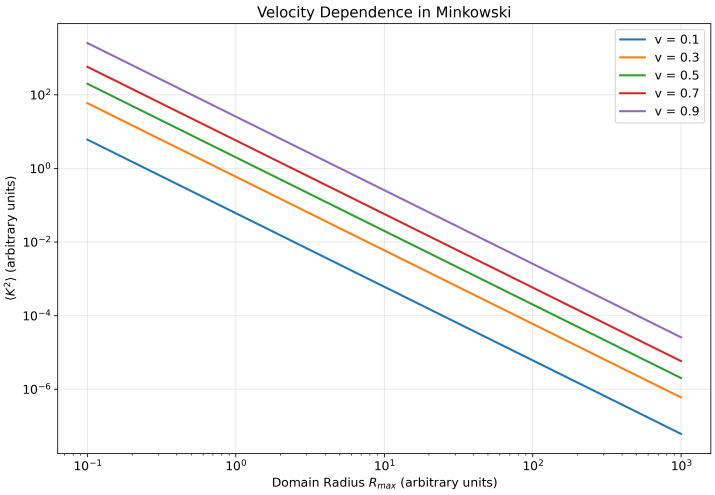

Figure 2: Dependence of $\langle K^2 \rangle$ on the foliation tilt parameter v in Minkowski spacetime (evaluated at finite infrared cutoffs). While the overall amplitude depends on v, the infrared decay with increasing $R_{\max}$ and the limit $\langle K^2 \rangle \to 0$ are universal, supporting the generic exclusion of Minkowski as an infrared vacuum for $K_0^2 > 0$.

This infrared scaling mechanism is qualitatively reminiscent of other approaches where large-scale (IR) effects can drive late-time acceleration without introducing a new local dark-energy field, albeit implemented here as a geometric selection rule rather than as a dynamical nonlocal modification of the field equations [6]. Therefore, for generic asymptotically flat foliations whose extrinsic curvature decays at large radius, Minkowski spacetime cannot satisfy the leafwise constraint $\langle K^2 \rangle_{D_\Theta} = K_0^2$ for any $K_0^2 > 0$. This result follows from the infrared scaling of the normalized average and is independent of the specific tilt parameters of the foliation. While special constant-mean-curvature or hyperboloidal slicings of flat spacetime may evade this argument by enforcing a non-vanishing extrinsic curvature through global boundary conditions, such configurations require fine-tuned foliation choices and do not arise generically from the infrared-dominated causal domains considered here. In this sense, Minkowski spacetime is not selected as a natural infrared vacuum by the leafwise geometric constraint.

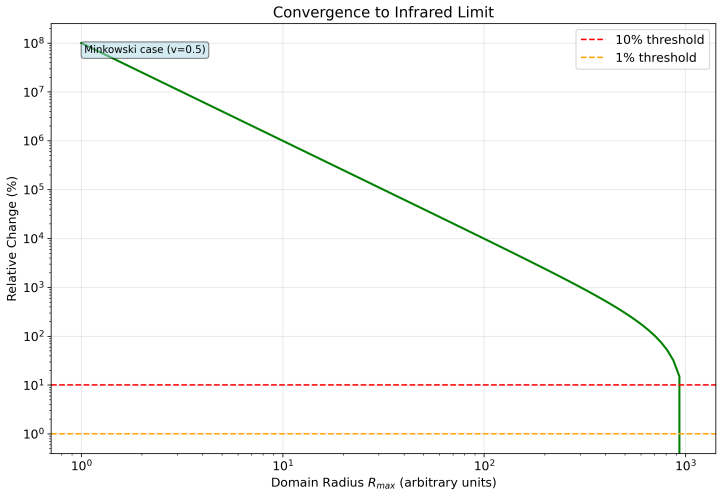

Figure 3: Convergence of the Minkowski leafwise average $\langle K^2 \rangle(R_{\max})$ toward its infrared limit (example shown for $v = 0.5$). The plot illustrates that a genuinely infrared domain is required for robust convergence, motivating the interpretation of the constraint as an infrared boundary condition defined by horizon-scale causal domains.

6.3 de Sitter spacetime

We next consider de Sitter spacetime in the static patch,

$$A(r) = 1 - H^2 r^2, \qquad B(r) = \left(1 - H^2 r^2\right)^{-1}. \tag{31}$$

For the Painlevé–Gullstrand slicing,

$$\psi'(r) = \frac{Hr}{1 - H^2 r^2}, \tag{32}$$

the kinetic invariant satisfies $X = 1$, and the squared extrinsic curvature of the Θ-hypersurfaces is constant,

$$K^2 = 3H^2. \tag{33}$$

Since K^2 is constant on the entire causal domain of the static patch, its normalized leafwise average coincides with the local value,

$$\langle K^2 \rangle_{D_\Theta} = 3H^2. \tag{34}$$

This step is certified in Lean by the de Sitter PG average theorem in `StaticSanityCheck/DeSitterPG.lean`.

It is worth noting that the causal domain of the de Sitter foliation is bounded by the cosmological horizon at $r = H^{-1}$, so that D_Θ has finite volume. The infrared limit defining the constraint is therefore saturated at

a finite, geometrically determined scale. This is in sharp contrast with the Minkowski case, where D_Θ extends to spatial infinity and the unbounded growth of the integration volume drives $\langle K^2 \rangle$ to zero. The vacuum selection mechanism can thus be traced to this structural asymmetry: de Sitter spacetime possesses a natural causal scale at which the constraint is intrinsically satisfied, whereas Minkowski spacetime lacks any such scale.

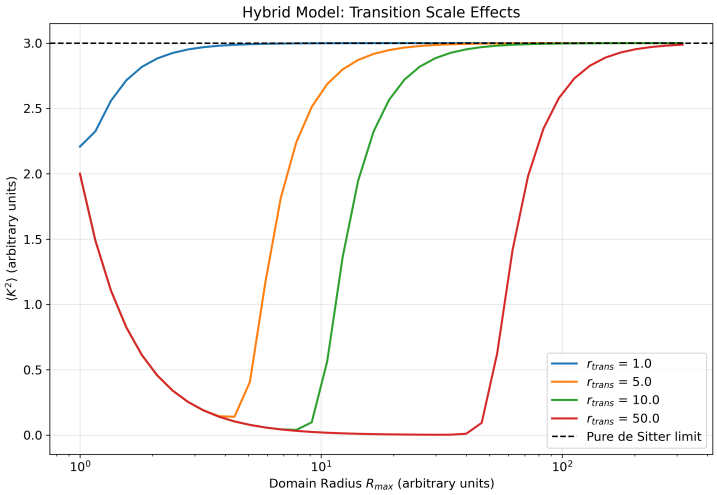

Figure 4: Hybrid toy model sensitivity: a Minkowski-like interior matched to a de Sitter exterior with transition radius r_{trans}. The leafwise average $\langle K^2 \rangle$ converges to the de Sitter value once the infrared domain extends well beyond the transition scale ($R_{\text{max}} \gg r_{\text{trans}}$), illustrating infrared dominance of the vacuum selection rule in inhomogeneous settings.

The leafwise constraint therefore selects de Sitter spacetime as an admissible vacuum, with the expansion rate fixed by

$$H^2 = \frac{K_0^2}{3}. \tag{35}$$

In the Lean artifact, this selection rule is proved both in the direct de Sitter module and in an independent module obtained by substitution into the general K^2 expression. This relation fixes the curvature scale of the *asymptotic* vacuum geometry selected by the leafwise constraint. Since the constraint is formally defined in the infinite-volume limit ($R \to \infty$), it does not impose a constant Hubble rate during the dynamical history at finite causal volume, where standard General Relativity is recovered. In the present case, the constancy of K^2 over the maximal causal domain ensures that the asymptotic average coincides with the pointwise value, providing a robust realization of the selected vacuum. More generally, however, the constraint requires only the global infrared average and does not enforce pointwise constancy of the extrinsic curvature.

6.4 Infrared dominance of the leafwise constraint

At this stage a potential concern may arise. Since the leafwise constraint fixes a non-zero value of the normalized average $\langle K^2 \rangle_{D_\Theta}$, one might worry that local Schwarzschild or post-Newtonian physics could be incompatible with the theory. This concern, however, relies on an incorrect interpretation of the constraint as a local condition.

The geometric constraint does not act pointwise on K^2, but only through its leafwise average over a causally defined domain. As a result, its effect is controlled by the large-scale structure of the foliation rather than by local curvature near compact sources. In the following we show explicitly that, for physically relevant foliations, the induced geometry on the $\Theta = \text{const}$ hypersurfaces remains locally Euclidean, ensuring full compatibility with standard Schwarzschild and post-Newtonian physics. The corresponding IR-suppression statement for compactly supported contributions is formalized in Lean as the compact-support IR-dominance theorem in `StaticSanityCheck/IRDominance.lean`.

Lemma 1 (Euclidean induced metric on the SdS–PG foliation)**.** *Consider the static Schwarzschild–de Sitter line element*

$$ds^2 = A(r)\,dt^2 - B(r)\,dr^2 - r^2 d\Omega^2, \qquad A(r) = 1 - \frac{2M}{r} - H^2 r^2, B(r) = \frac{1}{A(r)}. \tag{36}$$

Let the foliation be defined by the scalar field

$$\Theta(t, r) = t + \psi(r), \tag{37}$$

and choose the Painlevé–Gullstrand–type slicing

$$\psi'(r) = \frac{\sqrt{\frac{2M}{r} + H^2 r^2}}{A(r)}. \tag{38}$$

Then the metric induced on the hypersurfaces $\Sigma_\Theta : \Theta = \text{const}$ is exactly Euclidean:

$$\gamma_{ij}\,dx^i dx^j = dr^2 + r^2 d\Omega^2, \qquad \textit{hence} \qquad \sqrt{\gamma} = r^2 \sin\theta. \tag{39}$$

Proof. On a hypersurface $\Theta = \text{const}$ we have $d\Theta = dt + \psi'(r)\,dr = 0$, hence

$$dt = -\psi'(r)\,dr. \tag{40}$$

Substituting (40) into (36), the induced line element on Σ_Θ becomes

$$ds^2\big|_{\Sigma_\Theta} = \big(B(r) - A(r)\psi'(r)^2\big)\,dr^2 + r^2 d\Omega^2. \tag{41}$$

Using (38) and $B = 1/A$, we compute

$$B(r) - A(r)\psi'(r)^2 = \frac{1}{A(r)} - A(r)\,\frac{\frac{2M}{r} + H^2 r^2}{A(r)^2} = \frac{1 - \left(\frac{2M}{r} + H^2 r^2\right)}{A(r)}. \tag{42}$$

Finally, since $A(r) = 1 - \frac{2M}{r} - H^2 r^2$, the numerator in (42) equals $A(r)$ and therefore

$$B(r) - A(r)\psi'(r)^2 = \frac{A(r)}{A(r)} = 1. \tag{43}$$

Substituting (43) into (41) yields (39). □

As a consequence, the leafwise geometric constraint is dominated by the large-scale structure of the foliation, while local Schwarzschild and post-Newtonian physics remain unaffected. The apparent tension between the constraint and local gravity is therefore resolved at the geometric level.

7 Covariance and preferred foliation backgrounds

The formalism is generally covariant at the level of the action, but backgrounds for which $\nabla_\mu \Theta$ is timelike naturally select a preferred foliation of spacetime. This mechanism is conceptually related to those appearing in Einstein–Æther theories [1], Hořava–Lifshitz gravity [7], and khronometric models [3].

Although the foliation is defined by the gradient of a scalar field, the present framework differs from khronometric and scalar Einstein–Æther theories in a crucial way. The field Θ is not introduced as an independent dynamical degree of freedom with its own kinetic couplings, but serves a purely geometric role in defining the hypersurfaces on which the global constraint acts. Related scalar-aether and khronometric constructions, used for comparison, are discussed for instance in [4, 8]. The scalar field Θ is not introduced as an independent propagating degree of freedom describing new local physics. Instead, it serves a geometric role in defining the preferred foliation on which the global constraint acts. While a kinetic term is included in the local action, its role is to ensure the timelike character and regularity of the foliation, rather than to introduce an additional dynamical scalar mode in the infrared regime considered here.

The breaking of local Lorentz symmetry is therefore spontaneous rather than fundamental. The action remains fully diffeomorphism invariant, while specific solutions dynamically single out a preferred time direction through the gradient of Θ. In this sense, the preferred foliation does not represent a violation of covariance at the level of physical laws, but emerges as a property of the vacuum geometry selected by the leafwise constraint.

8 Perturbative completion and EFT regime

The perturbative sector is now implemented as an explicit pipeline in `Paper/Perturbative_Spectrum_Study/`, with corresponding script/log artifacts summarized in Sec. 9.

8.1 Quadratic operator and spin decomposition

The quadratic 4D operator is organized in Barnes–Rivers projectors as

$$\mathcal{O}_{4D} = c_2 P_2 + c_1 P_1 + c_s P_{0s} + c_w P_{0w} + c_m (P_{0sw} + P_{0ws}), \tag{44}$$

with closed-form inverse

$$\mathcal{O}_{4D}^{-1} = \frac{P_2}{c_2} + \frac{P_1}{c_1} + \frac{c_w P_{0s} + c_s P_{0w} - c_m (P_{0sw} + P_{0ws})}{c_s c_w - c_m^2}, \tag{45}$$

provided $c_2 \neq 0$, $c_1 \neq 0$, and $c_s c_w - c_m^2 \neq 0$. This algebraic closure and inversion are verified in `Paper/Perturbative_Spectrum_Study/scripts/12_full4d_spin_projector_inversion.wl`.

At coefficient level, the implemented structure is

$$c_A = c_A^{\mathrm{loc}} + c_A^{\mathrm{NL}} + \Delta c_A^{\mathrm{gf}}, \qquad A \in \{2, 1, s, w, m\}, \tag{46}$$

where c_A^{NL} is obtained from the covariant ratio expansion and Δc_A^{gf} is included through the gauge-fixing shifts used in `Paper/Perturbative_Spectrum_Study/scripts/14_full4d_covariant_gauge_fixed_coefficients.wl`. The current closure is therefore operational/parametric on the gauge-fixing projection side, while remaining fully explicit for the non-local variational block.

8.2 Dispersion relations and residues

For tensor and vector channels,

$$x_T = \frac{q^2 g_2 + m_T^2}{c_2}, \qquad x_V = \frac{q^2 g_1 + m_V^2}{c_1}, \tag{47}$$

while scalar modes follow from

$$\det\big[x K_s - (q^2 G_s + M_s)\big] = 0, \qquad K_s = \begin{pmatrix} c_s & c_m \\ c_m & c_w \end{pmatrix}. \tag{48}$$

The full dispersion/residue map, UV matching to Eigenvalues$(K_s^{-1} G_s)$, and positivity checks on tested samples are implemented in `Paper/Perturbative_Spectrum_Study/scripts/13_full_spectrum_dispersion_residues.wl` and `Paper/Perturbative_Spectrum_Study/scripts/09_vector_sector_full_stability_map.wl`.

8.3 Operational EFT validity window

The EFT diagnostics are defined in `Paper/Perturbative_Spectrum_Study/scripts/15_eft_validity_scales_proxy.wl` through

$$\epsilon_2 = \left| \frac{c_2^{\mathrm{NL}}}{c_2^{\mathrm{IR}}} \right|, \quad \epsilon_1 = \left| \frac{c_1^{\mathrm{NL}}}{c_1^{\mathrm{IR}}} \right|, \quad \epsilon_S = \frac{\|K_{\mathrm{NL}}\|_2}{\|K_{\mathrm{IR}}\|_2}, \tag{49}$$

with numerical scaling $\epsilon \sim L^{-3}$ in the tested IR sequence $L = \{10, 20, 40\}$. Strong-coupling proxies use kinetic gaps z_T, z_V, $z_{S,\min}$ and inverse residues z_T^{-1}, z_V^{-1}, $\lambda_{\max}(K_s^{-1})$, which remain finite and $\mathcal{O}(1)$ in the tested domain.

The tested momentum grid is $q^2 \in \{0.1, 1, 4\}$, with positive dispersion in all channels across sampled stable points. We therefore report $q^2_{\text{cut,proxy}} = 4$ as an *operational tested bound*, not as a fundamental UV cutoff of the theory.

8.4 Barotropic hard-constraint check (brief)

A dedicated FRW barotropic consistency test is included in `Paper/Barotropic_Cosmology_Study/scripts/00_barotropic_hard_constraint_consistency.wl`. It confirms that on the hard branch $H_0^2 = K_0^2/3$ the matter sector is absorbed in the leafwise multiplier $\lambda(t)$, with $\lambda'(t) = 0$ for $w = -1$ and generally $\lambda'(t) \neq 0$ for $w \neq -1$. This is consistent with the geometric vacuum-selection mechanism and is used here as a structural cross-check, not as a full realistic late-time cosmological fit.

9 Computational details

All symbolic checks were executed with *Wolfram Mathematica* v. 14.3. The computational artifact is organized into three audited pipelines:

1. **Variational derivation**: `Paper/Variational_Derivation/` (scripts `00..25`, logs, notebook exports). This block covers first/second variation of I_1/I_0, finite-domain boundary terms, FRW minisuperspace consistency, Noether/Bianchi identities, and covariant 4D bulk+boundary decomposition.

2. **Perturbative spectrum**: `Paper/Perturbative_Spectrum_Study/` (scripts `00..15`, logs, notebook exports). This block covers tensor/vector/scalar stability criteria, spin-projector algebra, 4D operator inversion, full dispersion/residue map, and EFT proxy diagnostics.

3. **Barotropic consistency check**: `Paper/Barotropic_Cosmology_Study/` (script `00`, log, notebook export). This block provides the hard-constraint FRW cross-check with barotropic matter.

Each folder includes a reproducible launcher (`run_all.ps1`) and explicit logs in `logs/`. For the current dataset, all reported pipeline checks are positive in their respective logs.

Traceability matrix (claim → files).

1. Covariant 4D variation and bulk+boundary split: `Paper/Variational_Derivation/scripts/23_covariant_causal_domain_variation.wl`,

Paper/Variational_Derivation/scripts/24_covariant_boundary_shape_derivative.wl, Paper/Variational_Derivation/scripts/25_covariant_nonlocal_action_variation.wl.

2. Finite-domain ratio/constraint checks: Paper/Variational_Derivation/scripts/12_finite_domain_ratio_variation.wl, Paper/Variational_Derivation/scripts/14_constraint_finite_domain_boundary.wl.

3. FRW constraint propagation and minisuperspace closure: Paper/Variational_Derivation/scripts/16_frw_minisuperspace_eom.wl, Paper/Variational_Derivation/scripts/17_frw_linearized_constraint_channel.wl, Paper/Variational_Derivation/scripts/18_desitter_constraint_propagation.wl, Paper/Variational_Derivation/scripts/19_frw_linearized_full_eom_reduction.wl, Paper/Variational_Derivation/scripts/20_minisuperspace_noether_bianchi_identity.wl, Paper/Variational_Derivation/scripts/22_frw_curvature_noether_identity.wl.

4. Quadratic non-local kernel from first principles ($\{a, b, A, B\}$ map): Paper/Perturbative_Spectrum_Study/scripts/10_first_principles_abAB_map.wl.

5. 4D projector algebra and inverse operator: Paper/Perturbative_Spectrum_Study/scripts/12_full4d_spin_projector_inversion.wl.

6. Full tensor/vector/scalar dispersion and residues: Paper/Perturbative_Spectrum_Study/scripts/13_full_spectrum_dispersion_residues.wl, Paper/Perturbative_Spectrum_Study/scripts/09_vector_sector_full_stability_map.wl.

7. Gauge-fixed coefficient assembly (operational/parametric closure): Paper/Perturbative_Spectrum_Study/scripts/14_full4d_covariant_gauge_fixed_coefficients.wl.

8. EFT validity proxies (IR scaling, strong-coupling diagnostics, operational tested cutoff): Paper/Perturbative_Spectrum_Study/scripts/15_eft_validity_scales_proxy.wl.

9. Barotropic hard-constraint cross-check: Paper/Barotropic_Cosmology_Study/scripts/00_barotropic_hard_constraint_consistency.wl.

9.1 Formal verification artifact (Lean)

The Lean formalization used in this work is publicly available and version-pinned for reproducibility:

- Repository: GitHub repository
- Artifact release used for this manuscript: `v2.0` release snapshot
- Archived DOI: `10.5281/zenodo.18361297`
- Continuous integration build: CI workflow

For referee traceability, the artifact README provides a mapping from paper equations to Lean theorems, with assumptions: README traceability table.

9.2 Scope of formal verification (explicit boundaries)

For precision, we state explicitly what is and is not currently certified in the Lean development associated with this work.

Starting point for K^2. The Lean proofs certify the full analytic chain *starting from* the explicit coordinate expression

$$K^2_{\text{general}} = \frac{\text{NumK2}}{\text{DenK2}},$$

and all substitutions/limits built on top of it (Minkowski IR scaling, de Sitter selection, abstract averaging lemmas, and IR-dominance statements). At present, the Lean code does *not* yet include a complete differential-geometric derivation of this coordinate formula from first principles (u^μ, projectors, connection, and tensorial construction of $K_{\mu\nu}K^{\mu\nu}$).

Causal domain D_Θ. In Lean, the causal domains are formalized via nested proxy families suitable for infrared analysis (balls B_R, and in de Sitter $B_{\min(R,H^{-1})}$), for which well-posedness, positivity of the normalization denominator, and finite-radius saturation are proved. What is not yet formalized is the full Lorentzian definition of mutual causal reachability and a general theorem proving equivalence between that definition and the proxy domains in all backgrounds.

Accordingly, statements of formal certification should be read with the following canonical scope: *The Lean artifact verifies the analytic chain of results starting from the explicit coordinate expression $K^2_{general}$ and the proxy domains used in the manuscript; it does not yet certify the derivation of $K^2_{general}$ from the full geometric definition $K_{\mu\nu}K^{\mu\nu}$, nor the equivalence between the proxy domains and the general Lorentzian causal-domain definition.*

Variational/perturbative computational scope. The extended pipelines in `Paper/Variational_Derivation/`, `Paper/Perturbative_Spectrum_Study/`, and `Paper/Barotropic_Cosmology_Study/` are reproducible symbolic/numeric checks with explicit logs, but are not yet fully imported into the Lean formalization.

Reproducibility note. Build verified for artifact release `v2.0` with Lean `v4.27.0` / mathlib `a3a10db0e9d66acbebf76c5e6a135066525ac900`; CI reproduces `lake build` on every push.

10 Conclusion

We have developed and checked a complete consistency chain for geometric vacuum selection from constrained spacetime foliations. The non-local leafwise condition on $\langle K^2 \rangle$ selects de Sitter in the infrared, excludes generic Minkowski asymptotics for $K_0^2 > 0$, and fixes the selected vacuum scale through

$$H^2 = \frac{K_0^2}{3}. \tag{50}$$

At the same time, local GR is recovered because non-local corrections are suppressed by inverse leafwise volume.

Beyond the background selection result, the present manuscript now includes: (i) explicit covariant variational control of the non-local action with bulk+boundary decomposition and second-order ratio expansion, (ii) full perturbative tensor/vector/scalar treatment with spin-projector operator inversion, dispersion relations, and residues, and (iii) an operational EFT validity analysis (IR scaling, proxy strong-coupling checks, and tested momentum window). A barotropic FRW hard-constraint study provides an additional structural cross-check of the branch mechanism.

The framework is therefore internally closed at variational and perturbative level. The remaining extensions are external/completion-level items: (1) gauge-independent BRST/Faddeev–Popov closure of the perturbative gauge-fixing sector, (2) fundamental UV completion beyond the operational tested cutoff, and (3) full observational inference in realistic cosmological histories.

These results support the interpretation of late-time acceleration as a global geometric property of foliation structure, rather than as a separate local dark energy degree of freedom.

References

[1] Ted Jacobson and David Mattingly. Gravity with a dynamical preferred frame. *Phys. Rev. D*, 64:024028, 2001.

[2] Ted Jacobson and David Mattingly. Static post-newtonian equivalence of general relativity and gravity with a dynamical preferred frame. *Phys. Rev. D*, 69:064005, 2004.

[3] Diego Blas, Oriol Pujolàs, and Sergey Sibiryakov. Consistent extension of hořava gravity. *Phys. Rev. Lett.*, 104:181302, 2010.

[4] Ted Jacobson and Eugene Lim. The scalar einstein-Æther theory. *Phys. Rev. D*, 90:024014, 2014.

[5] S.-Y. Pi. Space-times produced by a time-dependent scalar field. 2005.

[6] Nemanja Kaloper and Antonio Padilla. Vacuum energy sequestering: The framework and its cosmological consequences. *Phys. Rev. D*, 90:084023, 2014.

[7] Petr Hořava. Quantum gravity at a lifshitz point. *Phys. Rev. D*, 79:084008, 2009.

[8] Diego Blas et al. Slowly moving black holes in lorentz-violating scalar-tensor gravity. *Phys. Rev. D*, 111:024062, 2024.